RSC Advances

PAPER

View Article Online
View Journal | View Issue

Cite this: *RSC Adv.*, 2019, **9**, 16713

Robust fabrication of nanomaterial-based all-solid-state ion-selective electrodes

Kaikai Liu,[abc] Xiaojing Jiang,[bc] Yuehai Song*[a] and Rongning Liang *[bc]

Currently, nanomaterial-based all-solid-state ion-selective electrodes (ASS-ISEs) have become attractive tools for ion sensing in environmental and biological applications. However, nanomaterial solid contact can easily fall off the electrode surface owing to poor adhesion. This poses serious limits to the wide use of these sensors. Herein, we report a general and facile method for the robust fabrication of nanomaterial-based ASS-ISEs. It is based on the silver-based conductive adhesive (CA) with excellent electronic conductivity and strong adhesion ability as the binder to construct nanomaterial-based solid contact. The solid-contact Ca^{2+}-ISE based on single-walled carbon nanotubes (SWCNTs) is chosen as a model. The proposed electrode based on CA-SWCNTs shows a linear response in the concentration range of 10^{-6} to 10^{-3} M with a slope of 25.96 ± 0.36 mV per decade and a detection limit of 1.7×10^{-7} M. In addition, the CA-SWCNT-based Ca^{2+}-ISE exhibits an improved potential stability and reduced water film compared to the coated-wire ISE. Above all, experiments also show that the CA-SWCNT-based electrode exhibits nearly the same electrochemical characteristics as the classical only SWCNT-based electrode in term of resistance, capacitance and potential stability. We believe that CA-nanomaterial-based solid contacts provide an appealing substitute for traditional solid contacts based on nanomaterials.

Received 12th April 2019
Accepted 21st May 2019

DOI: 10.1039/c9ra02770j

rsc.li/rsc-advances

Introduction

In recent years, all-solid-state ion-selective electrodes (ASS-ISEs) have attracted considerable attention in ion sensing-related applications to clinical and environmental fields due to their attractive features including high portability, simplicity of use, affordability, and flexibility.[1–3] Nowadays, ASS-ISEs have shown exceptional promise for the construction of integrated devices, especially for wearable chemical sensors.[4,5] These electrodes have been recognized as the means by which the next ISE generation will be constructed. The coated-wire ISEs which are constructed by directly casting ISE membranes on the electronic conductors, are the simplest and the original form of ASS-ISEs.[6] However, the direct contact between the underlying electronic conductor and the sensing membrane may induce an unstable boundary potential response, because the blocked interface is unfavorable for the ion and electron transfers. A solid contact, which is placed between an electronic conductor and an ion-selective membrane, is regarded as the essential element for preparing a stable and reliable ASS-ISE. Actually, the presence of solid contact can largely improve the long-term stability and reproducibility of an ASS-ISE.[7]

Recently, nanostructured materials have been proposed as solid contacts,[8,9] such as three-dimensionally ordered macroporous (3DOM) carbon,[10] colloid-imprinted mesoporous (CIM) carbon,[11] carbon nanotubes,[12] graphene,[13] fullerence,[14] nanoclusters[15] and gold nanoparticles[16] owing to their intrinsic hydrophobicity and electric conductivity. These nanomaterial-based ISEs exhibit high potential stability and the absence of an interfacial aqueous layer between the sensing membrane and the underlying solid contact. Especially, these solid contacts have shown much more excellent resistance to O_2, CO_2, light and redox interferences than the classical conducting polymers.[17] These characteristics make these nanomaterials particularly suitable for their use in the fabrication of ASS-ISEs.

Generally, the nanomaterial-based solid contacts are prepared by the multilayer drop-casting methods.[12–16] However, it should be noted that the fabrication process is tedious. In addition, nanomaterials can easily fall off the electrode surface owing to the poor adhesion between these nanomaterials and the surface of metal substrate such as the glassy carbon electrode (GCE). Although poly(vinyl chloride) (PVC) has been successfully used as a facile and effective binder to fabricate the nanomaterial-based solid contact,[11] electrical conductivity of nanomaterial might be influenced by the PVC binder which is a non-conducting polymer. More recently, our group proposed

[a]*School of Environmental and Material Engineering, Yantai University, Yantai, Shandong 264005, P. R. China. E-mail: syuehai@163.com*

[b]*CAS Key Laboratory of Coastal Environmental Processes and Ecological Remediation, Yantai Institute of Coastal Zone Research, Chinese Academy of Sciences, Yantai, Shandong 264003, P. R. China. E-mail: rnliang@yic.ac.cn*

[c]*Shandong Key Laboratory of Coastal Environmental Processes, Yantai Institute of Coastal Zone Research, Chinese Academy of Sciences, Yantai, Shandong 264003, P. R. China*

a simple method for the fabrication of solid contacts based on nanomaterials. The ionic liquid, tetradodecylammonium tetrakis(4-chlorophenyl)borate (ETH 500), was used as binder.[18] Nevertheless, ETH 500 binder might also effect the original electroconductivity of nanomaterials since ETH 500 is not a room-temperature ionic liquid.

Herein, we report a general and facile method for fabricating the solid-contact ISEs based on nanomaterials as transducers. The electrically conductive adhesive, a glue that is commonly used for electronics applications, is used as a binder to fabricate nanomaterial-based solid contact. Such adhesive usually contains silver, graphite, or copper in an adhesive base that allow electrical current to pass through the adhesive. Since the conductive adhesive not only can provide strong adhesion between the GCE and nanomaterial but also has excellent electrical conductivity, it can be expected that the conductive adhesive will be used as an effective binder while keeping the excellent electroconductivity of nanomaterials unaffected. Particularly, the transducer layer can be prepared by simply spreading the conductive adhesive and nanomaterial composite on the GCE. In this work, single-walled carbon nanotubes (SWCNTs) have been chosen as a model of nanomaterials since they have been widely used as solid contacts of the ASS-ISEs. By using the proposed method, the all-solid-state Ca^{2+}-ISE based on the conductive adhesive/SWCNTs as solid contact has been developed. Experimental results show that the proposed approach offers a simple but robust way for fabrication of the nanomaterial-based ASS-ISEs.

Experimental section

Reagents and materials

Calcium ionophore (*N*,*N*-dicyclohexyl-*N*′,*N*′-dioctadecyl-3-oxapentanediamide, ETH 129), sodium tetrakis[3,5-bis(trifluoromethyl)phenyl]borate (NaTFPB), high molecular weight PVC and 2-nitrophenyl octyl ether (*o*-NPOE) were obtained from Sigma-Aldrich. SWCNTs were purchased from XFnano Materials Tech Co. Ltd (Nanjing, China). Conductive adhesive containing 30 wt% epoxy resin and 70 wt% silver powder was obtained from Xilite Adhesive Co. Ltd (Nanjing, China). Deionized water (18.2 MΩ cm specific resistance) obtained with a Pall-Cascada laboratory water system was used throughout. Tetrahydrofuran (THF) was freshly distilled prior to use. All other chemicals were of analytical reagent grade and used as received.

Preparation of solid contacts

GCE was firstly polished with 0.05 μm alumina slurries, and then rinsed with deionized water. After being cleaned by acetone, alcohol and deionized water successively, the obtained GCE was used as the electrode substrate. For preparation of the proposed solid contact, 2 mg of the conductive adhesive and 10 mg of SWCNTs were dispersed in 2 mL THF by sonication for 2 h, and then 50 μL of the obtained mixture was drop-cast onto the above polished GCE surface and dried by an infrared lamp. For comparison, the conventional SWCNTs-based solid-contact electrodes were prepared by the similar procedure except for omission of the conductive adhesive.

Fabrication of the all-solid-state Ca^{2+}-selective electrodes

The membrane cocktail components (totaling 360 mg), including ETH 129 (0.49 wt%), NaTFPB (0.46 wt%), PVC (33.02 wt%), and *o*-NPOE (66.03 wt%) were dissolved in 3.6 mL of THF. 90 μL of the membrane cocktail was drop-cast on to the transducer layer and allowed to dry for 6 h. As a comparison, the coated-wire Ca^{2+}-ISE was fabricated with the membrane cocktail directly casted on the polished GCE. Finally, all electrodes were conditioned in 1.0×10^{-3} M $CaCl_2$ overnight. The above prepared electrodes are denoted as GCE/conductive adhesive (CA)-SWCNTs/Ca^{2+}-ISE, GCE/SWCNTs/Ca^{2+}-ISE and GCE/Ca^{2+}-ISE.

Apparatus and measurements

The electromotive force (EMF) measurements were carried out at room temperature using a CHI 760C electrochemical workstation (Shanghai Chenhua Apparatus Corporation, China). The potentiometric assays were performed using a galvanic cell: Ag/AgCl (3 M KCl)/0.1 M LiOAc/sample solution/ISE membrane/nanomaterial layer/GCE. All EMF values were corrected for liquid junction potentials according to the Henderson equation, and activity coefficients were calculated according to the Debye–Hückel approximation.[19] Chronopotentiometry was carried out on the proposed all-solid-state Ca^{2+}-ISEs in 10^{-3} M $CaCl_2$ by applying a constant currents of ±1 nA for 60 s, respectively. Electrochemical impedance spectroscopy (EIS) measurements were performed by using a CHI 760C electrochemical workstation with a three-electrode configuration. The reference electrode was Ag/AgCl (3 M KCl), and the auxiliary electrode was a platinum wire. The impedance spectra were recorded at open-circuit potential in a solution of 0.1 M KCl with a frequency range of 0.3 Hz to 100 kHz and an amplitude of 10 mV. Scanning electron microscopy (SEM) images were obtained by using filed-emission scanning electron microscope (S-4800, Hitachi, Japan).

Results and discussions

Characterization of conductive adhesive/SWCNTs-based solid contact

In order to prevent nanomaterials falling off the electrode surface, nanomaterial-based solid contacts are often fabricated by drop-casting a mixture of conducting nanomaterials and non-conducting binder such as PVC, resulting in deterioration of their electrical properties. Here, we report a general method for fabrication of nanomaterial-based solid contacts. The transducer layer was simply prepared by drop-casting a mixture of conductive adhesive and SWCNTs. Since conductive adhesive has not only strong adhesion but also excellent electrical conductivity, a robust SWCNT-based ion-to-electron transducer with excellent electrochemical properties can be obtained. The surface morphology of the obtained solid contact was characterized by SEM. As shown in Fig. 1, the surface morphology of

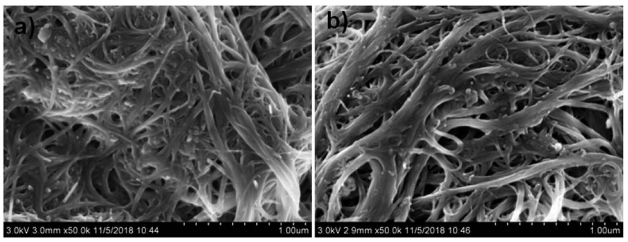

Fig. 1 SEM images of CA/SWCNT- (a) and SWCNT-based (b) solid contacts.

CA/SWCNT-based solid contact is only slightly different from that of SWCNT-based one. SWCNT-based solid contact exhibits an appearance of fiber-like wires with diameters of 10–100 nm, while CA/SWCNT-based one shows a more dense distribution of nanowires. Such slight difference can be mainly ascribed to the fact that wicking forces keep the conductive adhesive out of sight at the back at the nanotube/conductor interface.

Impedance measurements

The EIS measurements are used to characterize the proposed electrode. The impedance spectra of the GC/Ca^{2+}-ISE, GC/SWCNTs/Ca^{2+}-ISE and GC/CA-SWCNTs/Ca^{2+}-ISE, measured in 10^{-1} M KCl with a frequency range from 100 kHz to 0.03 Hz are shown in Fig. 2. As illustrated, all impedance spectra display a high-frequency semicircle which equals to the bulk membrane resistance coupled with the contact resistance at the interface between GC or solid contact and the ISE sensing membrane.[20] The resistance of the GC/CA-SWCNTs/Ca^{2+}-ISE (0.12 MΩ) is smaller than that of the GC/Ca^{2+}-ISE (0.28 MΩ), suggesting that the charge transfer across the interfaces is facilitated by CA-SWCNT-based solid contact. Additionally, it should be noted that, the GC/SWCNTs/Ca^{2+}-ISE exhibits a nearly same high-frequency resistance with the GC/CA-SWCNTs/Ca^{2+}-ISE (0.11 MΩ *vs.* 0.12 MΩ), which is probably due to the excellent electroconductivity of silver powder in the conductive adhesive. This result indicates that the presence of the conductive adhesive does not affect the charge transport ability of original SWCNTs. Here, note that, at high frequencies, high frequency artifacts which are the results of instrumental artifacts appear, when the impedance of the apparatus is comparable to or larger than the sample impedance.[21] Such apparatus might be further minimized by the appropriate corrections. Also, it is found that the GC/CA-SWCNTs/Ca^{2+}-ISE exhibits a similar low-frequency semicircle with GC/SWCNTs/Ca^{2+}-ISE but a much smaller one than the GC/Ca^{2+}-ISE, indicating that both solid contacts indeed promote the increase of low-frequency capacitance and facilitate the ion-to-electron transduction between the electrode substrate and the ISE membrane.[22,23]

Above all, addition of the conductive adhesive still does not change the low-frequency capacitance of classical SWCNT-based solid contact. Such unaffected effect both in the high-frequency and low-frequency semicircles can be attributed to the excellent electrical conductivity of the silver-based conductive adhesive. Thus, it can be expected that CA-SWCNT-based solid contact will function well in the area of the ASS-ISEs and similar to conventional SWCNT-based solid contact.

Effects of oxygen, CO_2 and light

It has been well established that O_2 could change the phase boundary potential through forming an oxygen half-cell at the surface of electronic conductor, while CO_2 would affect the pH of the water layer between the ion-selective membrane and the electronic conductor and thus induce the potential drift.[24] Note that, previous reports have revealed that some carbon nanomaterial-based solid contacts, such as CIM carbon[11] and SWCNTs,[12] have no oxygen, CO_2 and light sensitivity because of their inert characteristics.[9] Since CA-SWCNT-based solid contact is a mixture of carbon nanomaterial and silver powder-based adhesive, it is necessary to examine the effects of oxygen, CO_2 and light.

The influences of O_2 and CO_2 on the potential stability of the proposed all-solid-state Ca^{2+}-ISE were investigated by purging the gases successively in 10^{-3} M $CaCl_2$. The results are shown in Fig. 3. It can be seen that there are no obvious potential changes

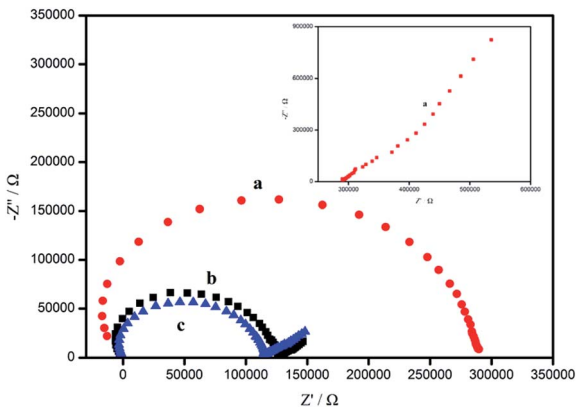

Fig. 2 Impedance spectra date for the proposed Ca^{2+}-ISE based on GC/Ca^{2+}-ISE (a), GC/CA-SWCNTs/Ca^{2+}-ISE (b) and GC/SWCNTs/Ca^{2+}-ISE (c). The inset is for the low frequency data of line (a).

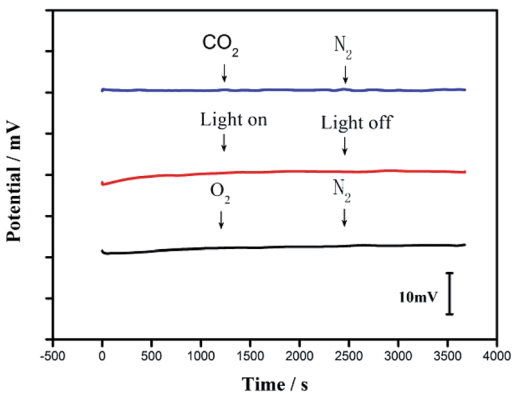

Fig. 3 Effects of O_2, CO_2 and light on the potential stability of the GC/CA-SWCNTs/Ca^{2+}-ISE in 1.0 × 10^{-3} M $CaCl_2$.

during the measurements, indicating that the GC/CA-SWCNTs/Ca^{2+}-ISE is insensitive to the interferences of both O_2 and CO_2. This is probably attributed to the fact that the embedment of silver powder into a resin adhesive prevents the reaction between silver and the gases (*e.g.*, O_2 and CO_2). Such stability can also be confirmed by the light sensitivity test in which the potentials were recorded while immersing the fabricated GC/CA-SWCNTs/Ca^{2+}-ISE into 10^{-3} $CaCl_2$ in the presence and absence of the ambient light. As expected, there are also no significant potential changes during the measurements.

Chronopotentiometry

Current-reversal chronopotentiometry was used to evaluate the short-term potential stability of the CA/SWCNTs-based Ca^{2+}-ISE. Fig. 4 shows the typical chronopotentiograms for both the GC/CA-SWCNTs/Ca^{2+}-ISE and GC/SWCNTs/Ca^{2+}-ISE. According to the ratio of $\Delta E/\Delta t$, the potential stability of the GC/CA-SWCNTs/Ca^{2+}-ISE is calculated to be ($5.4\ \mu V\ s^{-1}$, line a in Fig. 4), which is much lower than that of the GC/Ca^{2+}-ISE ($372\ \mu V\ s^{-1}$, line c in Fig. 4) under the same conditions. These results suggest that the presence of the CA-SWCNTs composite between the GC electrode and the Ca^{2+}-selective membrane indeed significantly improves the potential stability of the ASS Ca^{2+}-ISE. In addition, the potential stability of the proposed electrode is comparable to that of the SWCNT-based electrode (line b in Fig. 4). The high stability can be attributed to the high double layer capacitance of SWCNTs.

Potentiometric measurements

The potentiometric response of the GC/CA-SWCNTs/Ca^{2+}-ISE was measured in $CaCl_2$ in the concentration range of 1.0×10^{-8} to 1.0×10^{-3} M. Fig. 5A shows the time trace of the EMF response of the GC/CA-SWCNTs/Ca^{2+}-ISE. As illustrate, the electrode exhibits a stable potential response with a rapid response time of 10–15 s. The electrode shows a Nernstian response with a slope of 25.96 ± 0.36 mV per decade ($n = 3$) in the range from 10^{-6} M to 10^{-3} M with a detection limit of 1.7×10^{-7} M. In addition, it can be also seen that the proposed electrode functions equivalently, in terms of the calcium response, to the conventional SWCNT-based ISE with a detection limit of 3.1×10^{-7} M (Fig. 5B). The obvious drifts of potential signals for higher concentrations (*e.g.*, 10^{-3} M) in Fig. 5A are probably due to the perturbations from sample additions. Thus, it can be demonstrated that the introduction of the ion-to-electron transducer based on CA/SWCNTs does not affect the potential response performance of the solid-contact ISE.

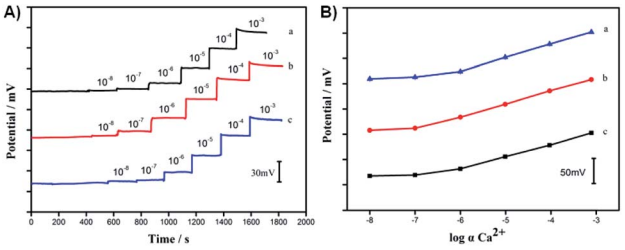

Fig. 5 Time traces (A) and calibration curves (B) of the GC/Ca^{2+}-ISE (a), GC/CA-SWCNTs/Ca^{2+}-ISE (b) and the GC/SWCNTs/Ca^{2+}-ISE (c) in $CaCl_2$ in the concentration range of 10^{-8} to 10^{-3} M.

Water layer test

It is well known that the formation of water layer between the ion-selective membrane and electrode substrate may cause the long-term instability of the ASS-ISEs since the composition can be changed by the re-equilibration of ions or some gases (*e.g.*, O_2 and CO_2) across the sensing membrane.[25] Hence, the classical potentiometric water layer test was performed to investigate the influence of a water film between the solid-contact layer and the Ca^{2+}-selective membrane. Fig. 6 exhibits the potential response of the proposed Ca^{2+}-ISE based on CA/SWCNTs and the coated wire GC/Ca^{2+}-ISE measured in 10^{-3} M $CaCl_2$, 10^{-3} M NaCl and again 10^{-3} M $CaCl_2$, respectively. Clearly, the positive drift in interfering NaCl solution is observed for the GC/Ca^{2+}-ISE without solid contact, and there is a negative potential drift when the sample solution is changed back to the NaCl solution. These potential drifts can be attributed to the presence of an aqueous layer between GC and ISE membrane.[7] In contrast, no obvious potential drift can be observed for the proposed GC/CA-SWCNTs/Ca^{2+}-ISE when changing the electrode from

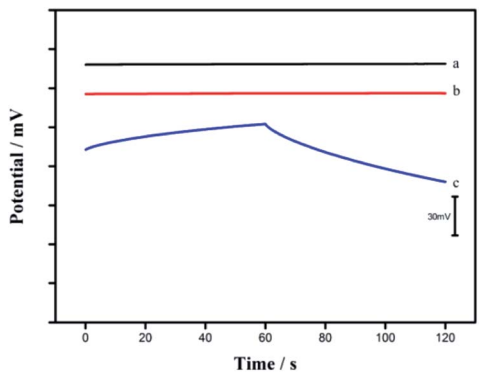

Fig. 4 Chronopotentiograms for GC/CA-SWCNTs/Ca^{2+}-ISE (a), GC/SWCNTs/Ca^{2+}-ISE (b) and GC/Ca^{2+}-ISE (c) recorded in a 1.0×10^{-3} M $CaCl_2$ solution. Applied current, ±1 nA for 60 s, respectively.

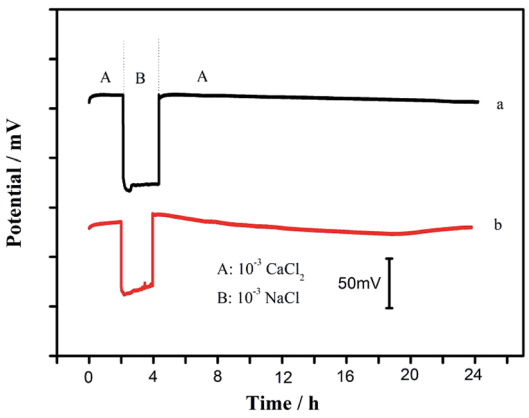

Fig. 6 Water layer tests for GC/CA-SWCNTs/Ca^{2+}-ISE (a) and GC/Ca^{2+}-ISE (b).

interfering ions NaCl to primary ions $CaCl_2$, indicating that the presence of CA-SWCNTs composite between the electrode substrate and the calcium-selective membrane can effectively avoid the formation of the undesirable water layer. This long-term stability of the proposed electrode might be due to the fact that the high lipophilicity of SWCNTs and the physically robust nature, good adhesion properties of the conductive adhesive prohibit the formation of detrimental water layer.[26] These results suggest that the proposed solid contact ISEs exhibit an excellent potential stability. In addition, the proposed sensor exhibits good reproducibility and long-term stability. For 10^{-5} M Ca^{2+}, the relative standard deviation of three electrodes was found to be 1.8%. No obvious change in Nernstian slope of the proposed electrode was observed after three weeks.

Conclusions

In this work, we report a general and facile method for fabricating the nanomaterial-based all-solid-state ISEs. The silver powder-based conductive adhesive with an excellent adhesion ability and a good electroconductivity is used as a binder to construct nanomaterial-based solid contact. Compared to the coated-wire ISE, the proposed solid-contact Ca^{2+}-ISE based on the conductive adhesive/SWCNTs exhibits significantly improved potential stability and long-term stability while keeping its excellent potential response properties. Above all, the conductive adhesive/SWCNT-based electrode shows the nearly same electrochemical characteristics with the classical only SWCNT-based electrode, such as resistance, capacitance and potential stability. Since many nanomaterials have been extensively exploited in ASS-ISEs,[8,9] this methodology can be extended to the development of other nanomaterial-based solid-contact ISEs. In view of the simple, robust and general nature of the proposed approach, it can be expected that the present work may pay the way to fabricating simple and robust all-solid-state nanomaterial-based potentiometric sensors for analysts. Note that, in this work, every electrode needs to be calibrated individually before each measurement. Such process is cumbersome and time consuming. This problem would be effectively resolved by using calibration-free solid-state potentiometric sensors pioneered by Bühlmann's group.[27]

Conflicts of interest

There are no conflicts to declare.

Acknowledgements

This work was financially supported by the National Natural Science Foundation of China (21874151, 41576106) and the Youth Innovation Promotion Association of CAS (2014190).

References

1 J. Bobacka, A. Ivaska and A. Lewenstam, *Chem. Rev.*, 2008, **108**, 329–351.
2 J. B. Hu, A. Stein and P. Bühlmann, *Trends Anal. Chem.*, 2016, **76**, 102–114.
3 K. Y. Chumbimuni-Torres, N. Rubinova, A. Radu, L. T. Kubota and E. Bakker, *Anal. Chem.*, 2006, **78**, 1318–1322.
4 A. J. Bandodkar, I. Jeerapan and J. Wang, *ACS Sens.*, 2016, **1**, 464–482.
5 W. Gao, S. Emaminejad, H. Y. Y. Nyein, S. Challa, K. Chen, A. Peck, H. M. Fahad, H. Ota, H. Shiraki, D. Kiriya, D. H. Lien, G. A. Brooks, R. W. Davis and A. Javey, *Nature*, 2016, **529**, 509–514.
6 R. W. Cattrall and H. Freiser, *Anal. Chem.*, 1971, **43**, 1905–1906.
7 M. Fibbioli, W. E. Morf, M. Badertscher, N. F. de Rooij and E. Pretsch, *Electroanalysis*, 2000, **12**, 1286–1292.
8 A. Düzgün, G. A. Zelada-Guillén, G. A. Crespo, S. Macho, J. Riu and F. X. Rius, *Anal. Bioanal. Chem.*, 2011, **399**, 171–181.
9 T. J. Yin and W. Qin, *Trends Anal. Chem.*, 2013, **51**, 79–86.
10 C. Z. Lai, M. A. Fierke, A. Stein and P. Bühlmann, *Anal. Chem.*, 2007, **79**, 4621–4626.
11 J. B. Hu, X. U. Zou, A. Stein and P. Bühlmann, *Anal. Chem.*, 2014, **86**, 7111–7118.
12 G. A. Crespo, S. Macho and F. X. Rius, *Anal. Chem.*, 2008, **80**, 1316–1322.
13 J. F. Ping, Y. X. Wang, J. Wu and Y. B. Ying, *Electroanal. Chem.*, 2011, **13**, 1526–1532.
14 M. Fouskaki and N. Chaniotakis, *Analyst*, 2008, **133**, 1072–1075.
15 M. Zhou, S. Gan, B. Cai, F. Li, W. Ma, D. Han and L. Niu, *Anal. Chem.*, 2012, **84**, 3480–3483.
16 E. Jaworska, M. Wójcik, A. Kisiel, J. Mieczkowski and A. Michalska, *Talanta*, 2011, **85**, 1986–1989.
17 J. Bobacka, *Electroanalysis*, 2006, **18**, 7–18.
18 R. N. Liang, T. J. Yin and W. Qin, *Anal. Chim. Acta*, 2015, **853**, 291–296.
19 S. Kamaata, A. Bhale, Y. Fukunaga and H. Murata, *Anal. Chem.*, 1988, **60**, 2464–2467.
20 J. F. Ping, Y. X. Wang, Y. B. Ying and J. Wu, *Anal. Chem.*, 2013, **84**, 3473–3479.
21 E. L. Anderson and P. Bühlmann, *Anal. Chem.*, 2016, **88**, 9738–9745.
22 J. Bobacka, A. Lewenstam and A. Ivaska, *J. Electroanal. Chem.*, 2000, **489**, 17–27.
23 J. P. Veder, R. De Marco, G. Clarke, R. Chester, A. Nelson, K. Prince, E. Pretsch and E. Bakker, *Anal. Chem.*, 2008, **80**, 6731–6740.
24 R. W. Cattrall, D. M. Drew and I. C. Hamilton, *Anal. Chim. Acta*, 1975, **76**, 269–277.
25 M. Fibbioli, K. Bandyopadhyay, S. G. Liu, L. Echegoyen, O. Enger, F. Diederich, D. Gingery, P. Bühlmann, H. Persson, U. W. Suter and E. Pretsch, *Chem. Mater.*, 2002, **14**, 1721–1729.
26 G. A. Crespo, S. Macho, J. Bobacka and F. X. Rius, *Anal. Chem.*, 2009, **81**, 676–681.
27 X. U. Zou, X. V. Zhen, J. H. Cheong and P. Bühlmann, *Anal. Chem.*, 2014, **86**, 8687–8692.